aerospace

MDPI

Article

The Development and Application of Two-Color Pressure-Sensitive Paint in Jet Impingement Experiments

Wei-Chieh Chen [1], Chih-Yung Huang [1,*], Kui-Thong Tan [2] and Hirotaka Sakaue [3]

[1] Department of Power Mechanical Engineering, National Tsing Hua University, Hsinchu 30013, Taiwan; weichiehchen@gapp.nthu.edu.tw
[2] Department of Chemistry, National Tsing Hua University, Hsinchu 30013, Taiwan; kttan@mx.nthu.edu.tw
[3] Department of Aerospace and Mechanical Engineering, University of Notre Dame, Notre Dame, IN 46556, USA; hsakaue@nd.edu
* Correspondence: cyhuang@pme.nthu.edu.tw

Abstract: This study aimed to develop a two-color pressure-sensitive paint (PSP) that has both high pressure sensitivity and high temperature sensitivity. Different nitrobenzoxadiazole (NBD) derivatives were used as the temperature probe. Among them, NBD-ZY37 demonstrated favorable stability against photodegradation, and its temperature sensitivity in an RTV118-based two-color PSP was −1.4%/°C. Moreover, temperature sensitivity was independent of pressure in the tested temperature range. PtTFPP was used, and its pressure sensitivity was measured to be 0.5% per kPa. The two-color PSP paint underwent further examination in jet impingement experiments. The experimental results indicated that the pressure fluctuation introduced by the shock waves occurred earlier at higher impingement angles. Specifically, when the pressure ratio was 2.38, increasing the impinging angle from 15° to 30° caused the location of the pressure wave to move from s/D at 0.8 to the exit of the nozzle. Simultaneously, the shape of the maximum pressure zone changed from a fan shape to a round shape. Additionally, the jet region expanded when the pressure ratio was increased.

Keywords: pressure-sensitive paint; two-color PSP; temperature correction; jet impingement

Citation: Chen, W.-C.; Huang, C.-Y.; Tan, K.-T.; Sakaue, H. The Development and Application of Two-Color Pressure-Sensitive Paint in Jet Impingement Experiments. *Aerospace* **2023**, *10*, 805. https://doi.org/10.3390/aerospace10090805

Academic Editor: Sergey Leonov

Received: 4 July 2023
Revised: 12 September 2023
Accepted: 13 September 2023
Published: 15 September 2023

1. Introduction

Surface-sensing techniques are crucial in aerospace research. Pressure-sensitive paint (PSP) and temperature-sensitive paint (TSP) serve as tools for measuring pressure and temperature sensing on global surfaces, and they are widely used in the field of aerospace engineering [1,2]. These techniques are characterized by their non-intrusive nature, allowing them to provide global pressure and temperature mapping across surfaces. PSP usually contains a single luminophore, which is sensitive to pressure and is dissolved in a polymer binder and solvent. However, a disadvantage of most PSPs is that they are sensitive not only to pressure but also to temperature. This dual sensitivity can lead to inaccurate pressure readings as the pressure profile may be affected by temperature variations. Therefore, correcting for the temperature effect is essential to obtain accurate pressure data. A straightforward approach to rectifying the pressure readings is to acquire a corresponding temperature profile. Both TSP and PSP can be used simultaneously to test symmetry models [3], enabling the correction of temperature effects using the temperature profile obtained from TSP. However, the applicability of this method is limited by the shape of the models under study.

Two-color PSP has been developed to simultaneously acquire temperature and pressure data. By spraying PSP and TSP at different layers, both the pressure and temperature data can be obtained concurrently [4,5]. A thin layer of clear paint is positioned between PSP and TSP to prevent chemical reactions and fluorescence resonance energy transfer (FRET). However, positioning the TSP layer as the lower layer can result in a weak signal, causing the temperature readings to differ slightly from the PSP layer. Thus, these temperature

differences can affect the temperature correction, which reduces accuracy. Another method involves printing TSP and PSP in a grid array using an inkjet printer [6,7]. Although this method allows image acquisition through a monochrome camera, the preparation of the dual-sensor arrays is more complex. Also, poor spatial resolution can complicate the analysis, and the edge of the dot may include inaccurate intensity ratios that must be removed. The most common form of two-color PSP is dual-luminophore paint [8–10], a combination of PSP and TSP sensors. This system functions based on a mixture of two different luminophores with different emission bands. By separating these bands, the PSP and TSP signals can be acquired using a color CCD or a monochrome CCD equipped with a filter wheel containing multiple filters. The temperature-sensitive luminophore must exhibit strong temperature sensitivity without being influenced by pressure. However, FRET often occurs in two-color PSP due to spectrum overlapping, and the two luminophores usually must have an overlapped absorption spectrum if a single excitation is preferred. Iijima et al. used PtTFPP as the pressure sensor and poly(1-trimethylsilyl-1-propyne) (PTMST) as the temperature sensor [11]. Their paint is easy to prepare, and the temperature sensor remains unaffected by pressure. In their study, the pressure sensitivity of the pressure probe was 0.4%/kPa, and the temperature sensitivity of the temperature probe was −0.5%/K. Although an overlapped emission band led to FRET, the signals from both probes could still be separated, demonstrating the potential of the dual-luminophore PSP as a temperature-corrected PSP. Beyond two-color PSP, other temperature-cancellation methods for PSP have been explored. Li et al. used the self-assembled monolayer technique to minimize the temperature effect on the PSP [12], and Gu et al. used comarin 6 and PtTFPP as luminophores with opposite temperature sensitivity to cancel the temperature effect [13]. In this study, we introduce a new combination of dual-luminophores and examine different formulations of two-color PSPs that use nitrobenzoxadiazole (NBD) derivatives as temperature dyes. These dyes were selected for their high-temperature sensitivity, lack of pressure dependency, and green channel emission bands (which are easily separable from the red channel). The two-color PSPs were also characterized.

The distribution of pressure on a surface with jet impingement can be acquired using the PSP technique [6,8,14]. More details can be captured through quantitative visualization with the PSP technique. With a strong pressure gradient, the capabilities of a two-color PSP can be demonstrated. Thus, the newly developed two-color PSP was applied to the jet impingement experiments in this study.

2. Materials and Methods

2.1. Materials

Platinum(II)-5,10,15,20-tetrakis-(2,3,4,5,6-pentafluorphenyl)-porphyrin (PtTFPP) served as the pressure-sensitive luminophore in this study. Chapman et al. and Fery-Forgues et al. have reported that NBD derivatives exhibit temperature dependency, but no study has used this luminophore in two-color PSP applications [15,16]. The excitation spectrum for NBD derivatives ranges from 422 to 482 nm, with the emission peak extending from 500 to 570 nm, depending on the solvents used. This emission light range fulfills the requirements for the two-color PSP. Toluene was chosen as the solvent due to its high quantum yield for NBD derivatives and its compatibility with PtTFPP. Four different temperature-related luminophores were used in the two-color PSP tests: 6-(N-(7-Nitrobenz-2-oxa-1,3-diazol-4-yl)amino)hexanoic acid (NBD-X), 4-Fluoro-7-nitrobenzofurazan (NBD-F), N-methyl-7-nitrobenzo[c][1,2,5]oxadiazol-4-amine (NBD-ZY36), and N,N-dimethyl-7-nitrobenzo[c][1,2,5]oxadiazol-4-amine (NBD-ZY37). In the two-color PSP characterization tests, two widely used polymer binders, RTV118 and poly(4-tert-butylstyrene) (Poly(tBS)), were selected and tested. For the formulations with RTV118 used as the binder, 50 mg of RTV118 was used. The binder comprised RTV118 and poly(tBS) that were mixed at a ratio of 3:2 by concentration. In the sample where only poly(tBS) was used, the formulation included 550 mg of poly(tBS). Silicon dioxide was exclusively used in one of the formulations

with NBD-X. A 4.0 cm × 4.0 cm aluminum square coupon was used for the characterization tests of the paints, and the paints were applied to the sample using a traditional airbrush.

2.2. Experiment Setup

The coupon sample was placed in a pressure chamber to test both pressure sensitivity and photodegradation, as depicted in Figure 1. The testing pressure range extended from 14.5 to 130.0 kPa. The same pressure calibration setup was used for the photodegradation experiments. During these tests, the pressure was maintained at 100.9 kPa, and the experiments were conducted in an air-conditioned lab at a controlled temperature of 25 °C. Temperature tests were performed in the temperature control chamber. As shown in Figure 2, the sample was placed in this chamber, and the temperature was varied between 15 °C and 40 °C. Reference conditions were set at 100.9 kPa and 25 °C. The sample was excited using 450 nm LED light, and the luminescent signals were recorded using two 14-bit CCD cameras: a mono CCD camera (PCO pixelfly, monochrome version) for the two-color PSP development stage and a color CCD camera (PCO pixelfly, color version) for the characterization of the chosen two-color PSP and subsequent jet impingement experiments. In terms of optical filter selection, a 600 nm long-pass filter was mounted on the mono CCD camera to capture pressure data, and a 525 ± 25 nm band-pass filter was used for the temperature-related signal. A dual band-pass filter (CHROMA ZET488/594m) was mounted on the color CCD to differentiate between pressure and temperature signals and reduce the effects of high quantum efficiency in the green spectrum. Additionally, a spectrometer (Ocean Optics USB2000) was positioned toward the experimental system to capture emissions during calibration experiments. This spectrometer was also used for pressure and temperature calibration by analyzing the emission spectra. The spectrometer, the CCD camera, and the LED excitation light were positioned around 52 cm from the chambers. The experimental setup for jet impingement experiments is presented in Figure 3. Dry air from a compressed air tank served as the test gas, and a 450 nm LED light excited the paint. The impingement surface was mounted on a three-axis translation stage, allowing for the adjustment of the impingement distance. The jet was set on a separate platform that enabled the adjustment of the impingement angle. Both the CCD and the excitation light were placed approximately 1 m in front of the testing sample. Figure 4 illustrates the geometry for the impinging jet, with an exit diameter of the nozzle at 2.7 mm and an impingement surface constructed from a 3.0 mm thick aluminum plate. Table 1 presents the conditions in the jet impingement experiments. The impingement and jet distance ratio (H/D) was fixed at 3.56, and three pressure ratios (Φ, P_0/P_∞) were used: 2.38, 3.40, and 4.42. For single luminophore-sensitive paint, PSP, and TSP, the impingement angle (α) was 20°. For the two-color PSP impingement test, the impingement angles (α) were 15°, 20°, and 30°.

Table 1. Test conditions for the impinging jet.

	Two-Color PSP (H/D = 3.56)			**PSP, TSP (H/D = 3.56)**
Φ		**α**		**α**
2.38	15°	20°	30°	20°
3.40	15°	20°	30°	
4.42	15°	20°	30°	

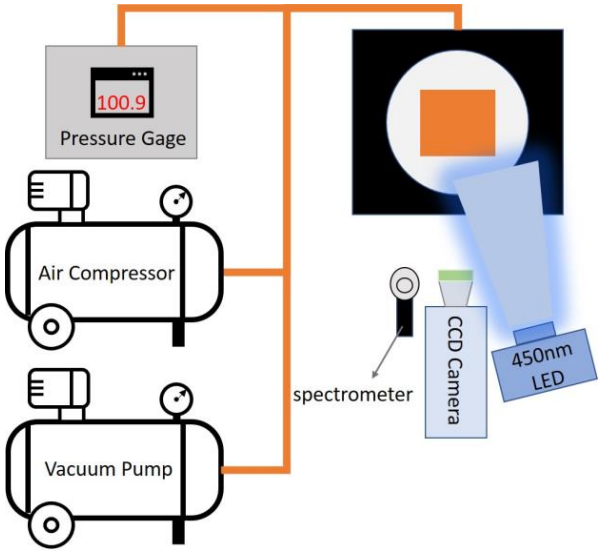

Figure 1. Pressure calibration setup.

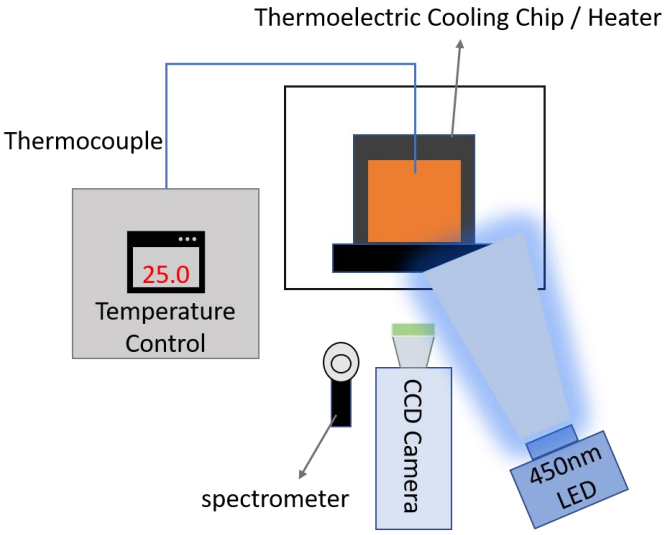

Figure 2. Temperature calibration setup.

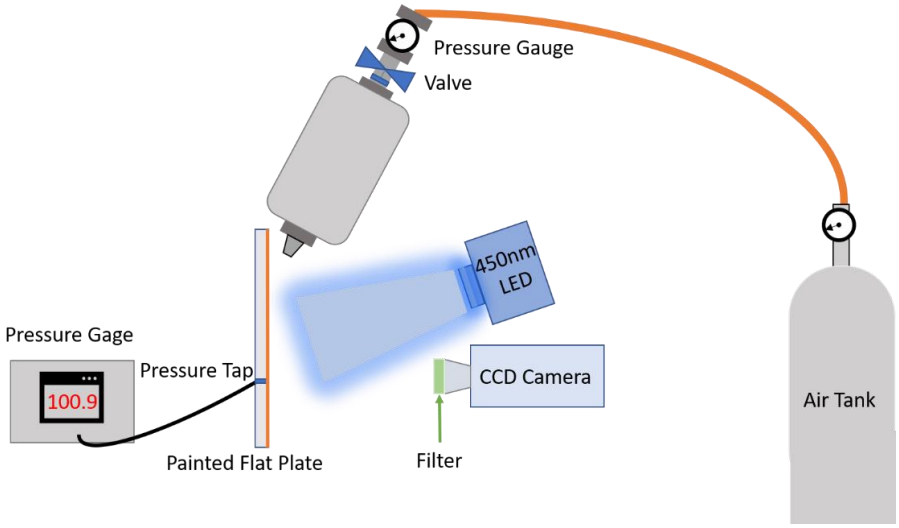

Figure 3. Jet impingement setup.

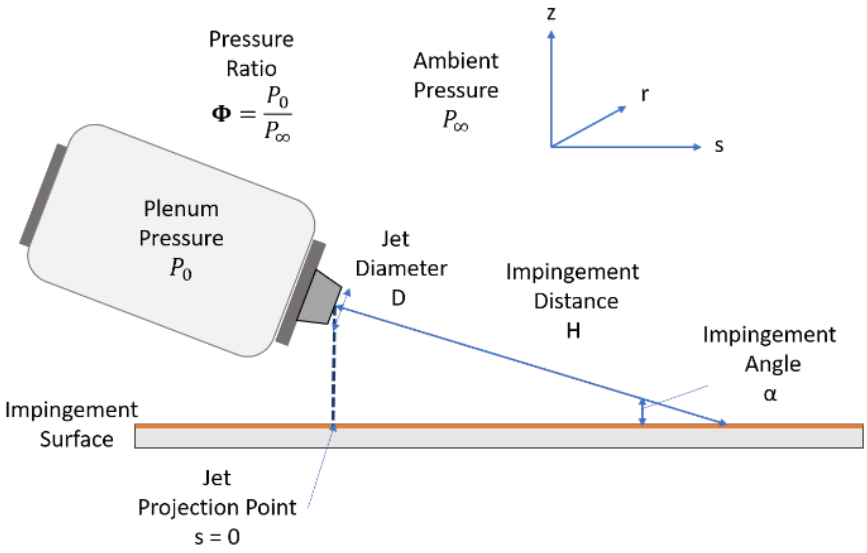

Figure 4. Geometry of the impinging jet.

2.3. Temperature Correction

In this study, an intensity-based calibration method was used. When the model's surface was illuminated by the excitation LED, two selected luminescence signals were emitted from the paint. Specifically, the green and red signals originated from the temperature and pressure probes, respectively. The intensity images corresponding to the pressure and temperature probes were acquired separately from the color CCD in the red and green channels. The luminescent intensity with respect to pressure, I_{ratio}, was determined using the Stern–Volmer equation [17]:

$$I_{ratio\_P} = \frac{I(P_{ref})}{I(P)} = f_1\left(\frac{P_{ref}}{P}\right) \tag{1}$$

For the temperature probe, the relationship is given as follows:

$$I_{ratio\_T} = \frac{I(T)}{I(T_{ref})} = f_2\left(\frac{T}{T_{ref}}\right) \tag{2}$$

Functions f_1 and f_2 are determined by the calibrations. Here, $_{ref}$ represents the reference images captured at ambient pressure and a temperature of 25 °C. For the temperature correction, a temperature correction function, c, was introduced in Equation (3) [8].

$$\frac{I_{ref}}{I} = \frac{I_{ratio\_P}}{\left(\frac{1}{I_{ratio\_T}} - 1\right) \times c(T) + 1} \tag{3}$$

where c is the ratio of the temperature sensitivity of the pressure probe and the temperature sensitivity of the temperature probe. In the context of the jet impingement experiments, the reference image was the wind-off image captured under uniform pressure and temperature conditions when the jet was turned off. $I(P)$ and $I(T)$ were the wind-on images under different experiment conditions obtained from the red channel and the green channel, respectively.

3. Results

3.1. Two-Color PSP Characterizations

The stability of the paint is a critical concern for the PSP. Accordingly, the photodegradation of the paints was examined. Table 2 presents a comparison of the photodegradation

of two-color PSP samples tested under 100.9 kPa and 25 °C. The photodegradation rate is defined in Equation (4).

$$\text{Photodegradation rate} = \frac{I_t - I_{t=0\text{min}}}{I_{t=0\text{min}}} \times 100\ [\%] \quad (4)$$

where I_t is the intensity at 60 or 120 min and $I_{t=0\text{min}}$ is the intensity at the starting time. Depending on the specific temperature-related luminophores used, the photodegradation rate of the temperature probe, as measured by the CCD camera, can reach up to 47% per hour. NBD-X has less photodegradation in the longer duration due to the speedy decay from the T probe. When the paint is exposed to the excitation light for a long time, the color of the paint changes from orange to pink. From this transition, it is obvious that the T probe dye has decayed, and the orange color from the T probe is fading. The signal from the T probe has been weakened, and the signal (pink color) from the P probe has dominated the signal output. The P probe has less photodegradation, which leads to the result that two-color paint has less photodegradation when it comes to the longer duration. After two hours, the photodegradation of the NBD-ZY36 sample reached 71%. Such severe photodegradation can decrease the signal-to-noise ratio of the paint and lead to fading of the paint color. Notably, two-color PSP with NBD-ZY37 had the lowest photodegradation rate, making it the preferred choice for the two-color PSP formulation. After selecting NBD-ZY37 as the temperature-related luminophore, different binder combinations were also tested.

Table 2. Photodegradation rates of two-color PSPs for comparison.

Photodegradation (%)								
T Probe Luminophore	**NBD-X**		**NBD-F**		**NBD-ZY36**		**NBD-ZY37**	
Time (min)	60	120	60	120	60	120	60	120
T probe (CCD)	46	43	39	49	47	71	5	13

Table 3 illustrates the sensitivity comparison of two-color PSP with different binders. These two-color PSPs display no pressure-related sensitivity but high-temperature dependency in the temperature probe. Two-color PSP with Poly(tBS) has a high-pressure sensitivity and low-temperature dependency in the pressure probe. Moreover, since temperature sensitivity was inhibited, the temperature sensitivity in both probes became similar. However, the binder itself can contribute to photodegradation.

Table 3. Sensitivity comparison of two-color PSP with different binders.

Binder	**RTV118**		**Poly(tBS)**		**Poly(tBS) Mixed RTV118**	
Probe	**P Probe**	**T Probe**	**P Probe**	**T Probe**	**P Probe**	**T Probe**
Pressure sensitivity (%/kPa)	0.5	−0.1	0.6	0.0	0.5	0.0
Temperature sensitivity (%/°C)	−2.6	−1.4	−0.9	−0.8	−2.3	−2.1

Table 4 compares the temperature probe photodegradation of two-color PSP with different binders. RTV118 had the lowest photodegradation rate, whereas poly(tBS) had the highest. As shown in Tables 3 and 4, the formula with poly(tBS) had higher pressure sensitivity and lower temperature sensitivity in the P probe, but it also exhibited low-temperature sensitivity in the T probe, and photodegradation was high. The mixed binder had a lower photodegradation rate than poly(tBS), and the temperature sensitivity of the pressure probe also decreased with the use of a mixed binder. Although the pressure sensitivity also decreased, the mixed binder could still inhibit the temperature sensitivity of the pressure probe. Nonetheless, the paint stability remained below that of

the two-color PSP with RTV118 used as the binder. Consequently, the two-color PSP with RTV118 demonstrated the best paint stability. Therefore, RTV118 was used as the binder in subsequent experiments.

Table 4. Temperature probe photodegradation comparison of two-color PSP with different binders.

Binder	RTV118		Poly(tBS)		Poly(tBS) Mixed RTV118	
Time (min)	60	120	60	120	60	120
T probe Photodegradation (%)	5	13	50	72	28	51

Figure 5 illustrates the pressure calibration in the spectrum. The green emission range (500–600 nm) represents the signal from the temperature-related dye, and the red emission range (600–750 nm) represents the signal from the pressure dye. As the pressure decreased, the emission from the pressure probe increased, and the temperature probe remained unaffected by changes in pressure. Figure 6 displays the emission spectra of the two-color PSP at different temperatures, revealing that temperature significantly affected both the pressure and temperature probes. Figure 7a provides the pressure calibration results from the spectrometer calibration system. The spectral integration for the P probe is from 605 nm to 750 nm, and for the T probe, it is from 500 nm to 575 nm. The pressure sensitivity from the temperature probe was 0.0%/kPa, indicating that it exhibited no pressure dependency. Conversely, the pressure sensitivity at the pressure probe was 0.6%/kPa. Figure 7b presents the temperature calibration results from the spectrometer calibration system. The temperature sensitivity at the pressure probe was −2.9%/°C, which was approximately twice the temperature sensitivity at the temperature probe. These results demonstrate that the temperature probe has the potential to function as a temperature sensor in the two-color PSP.

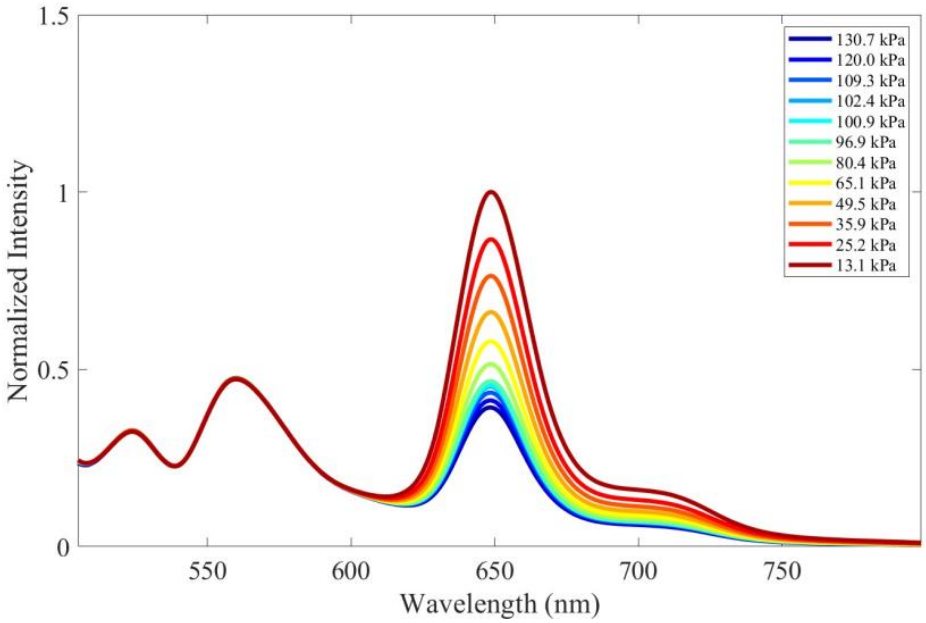

Figure 5. Pressure calibration in the spectrum.

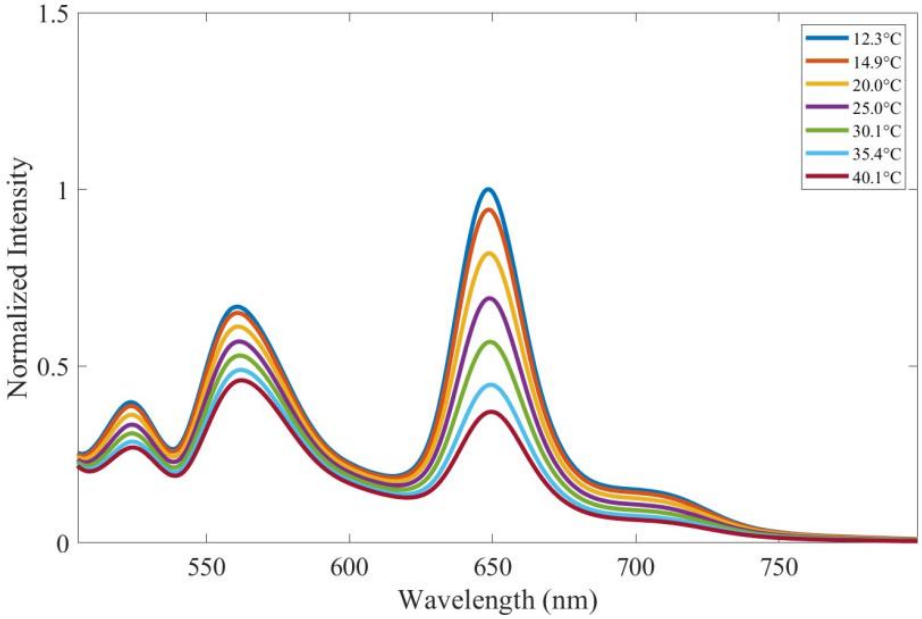

Figure 6. Emission spectra of two-color PSP at different temperatures.

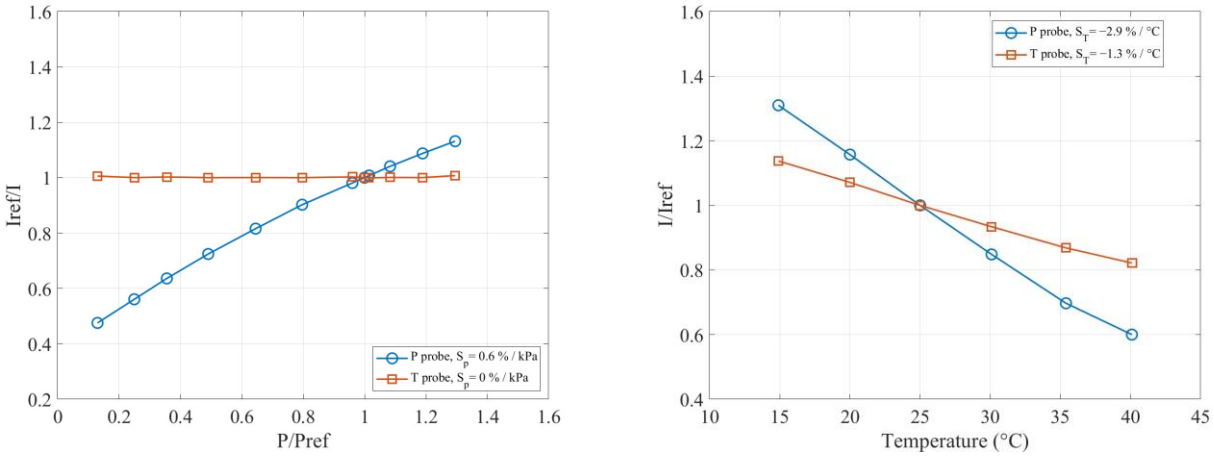

(**a**) (**b**)

Figure 7. Calibration results from the spectrometer calibration system. (**a**) Pressure calibration and (**b**) temperature calibration.

A comparison between monochrome and color CCD cameras is presented in Figure 8. Figure 8a shows the pressure calibration of a single luminophore PSP, revealing no differences between the results; both indicate a pressure sensitivity of 0.7%/kPa. Figure 8b displays the temperature calibration of a single luminophore PSP. Figure 9 provides the calibration curve of a single luminophore TSP, Figure 9a shows the pressure calibration, and Figure 9b shows the temperature calibration. The monochrome and color CCD cameras yield similar results for both single luminophore paints. Figure 10 depicts the pressure distribution on the surface and along the centerline, using a single luminophore PSP resulting from jet impingement (α = 20°, Φ = 3.40). Figure 11 illustrates the temperature distribution on the surface and along the center line using a single luminophore TSP under the same impingement conditions. Both CCD cameras exhibit a consistent correlation with each other. The pressure and temperature calibration curves of a two-color PSP using a color CCD camera are shown in Figure 12. The pressure sensitivity at the pressure probe is 0.5%/kPa, and at the temperature probe, it is −0.1%/kPa. Conversely, the temperature sensitivity at the pressure probe is −2.6%/°C, and at the temperature probe, it is

−1.4%/kPa. Slight differences exist between the spectrometer and CCD camera results, attributable to variations in the quantum yield of the color CCD camera across different emission ranges. Because the green channel extends over 600 nm, it might capture a portion of the emission signal from the pressure probe, subtly influencing the temperature result. However, this effect is nonsignificant in the pressure calibration of the temperature probe. From Figure 10, the pressure profile of jet impingement indicates that the pressure exceeds the calibration-tested pressure. This limitation is due to the constraints of the pressure chamber, where the pressure can go no higher than 130 kPa (Φ = 1.3). Consequently, the extrapolation method was used for pressures above the calibration-tested value, which might influence the accuracy of the results in this case. From the CCD camera noise, the sensor's error, and the error from the calibration curve, the uncertainty has been calculated as 2.03%.

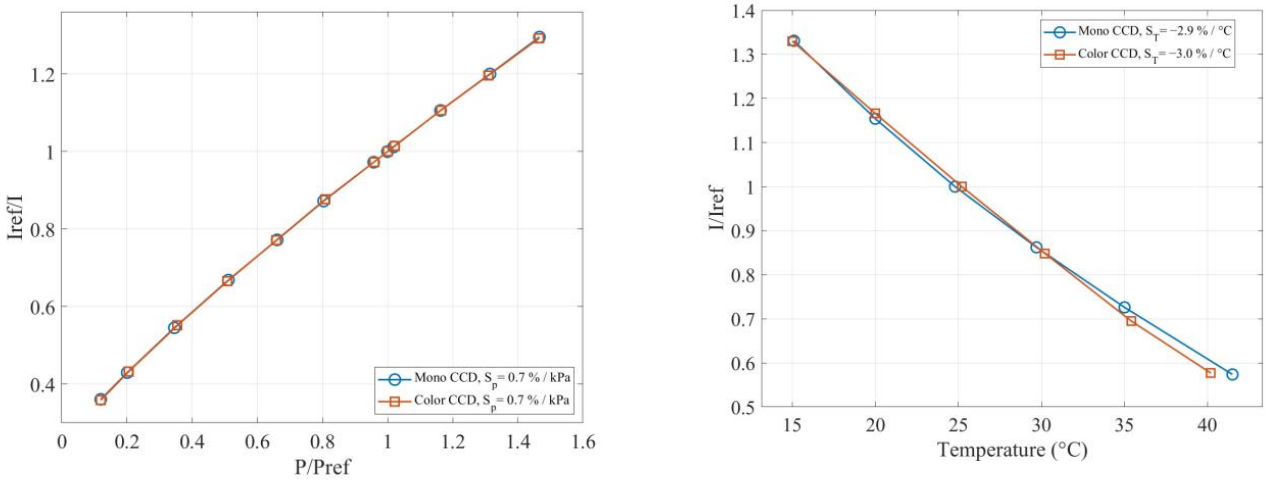

(**a**) (**b**)

Figure 8. (**a**) Pressure calibration of a single luminophore PSP and (**b**) temperature calibration of a single luminophore PSP from monochrome and color CCD camera for comparison.

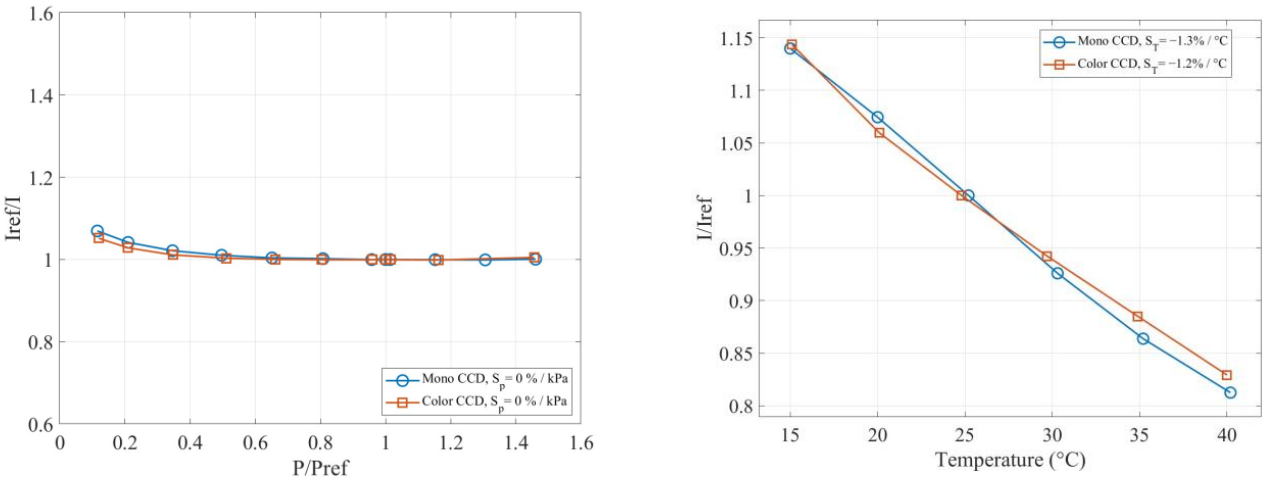

(**a**) (**b**)

Figure 9. (**a**) Pressure calibration of a single luminophore TSP and (**b**) temperature calibration of a single luminophore TSP from monochrome and color CCD camera for comparison.

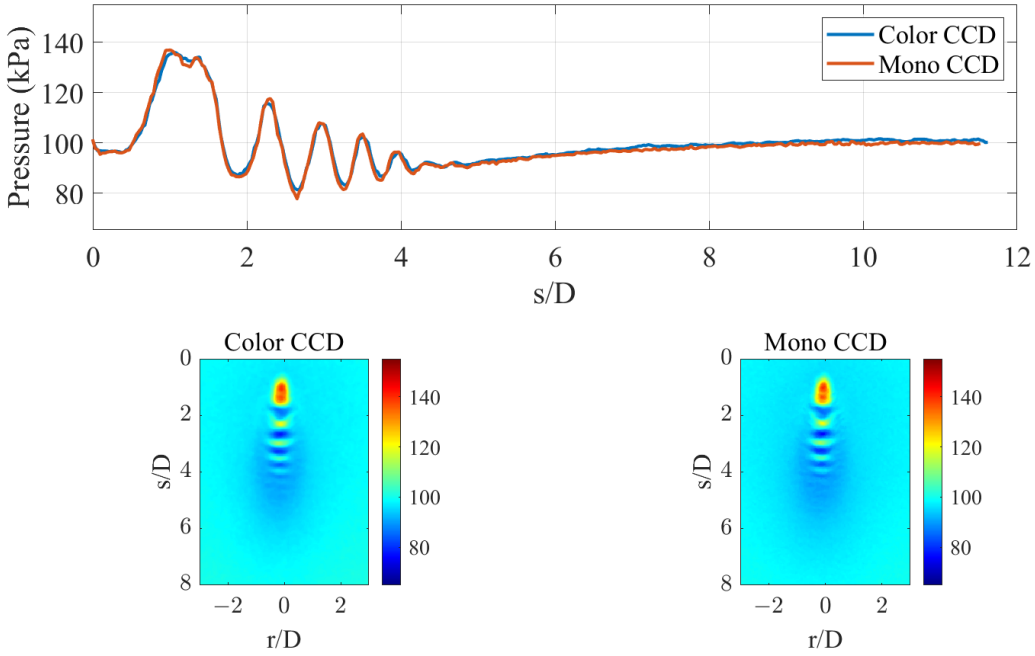

Figure 10. Description of pressure distribution on the surface and pressure along the centerline at $\alpha = 20°$ and $\Phi = 3.40$.

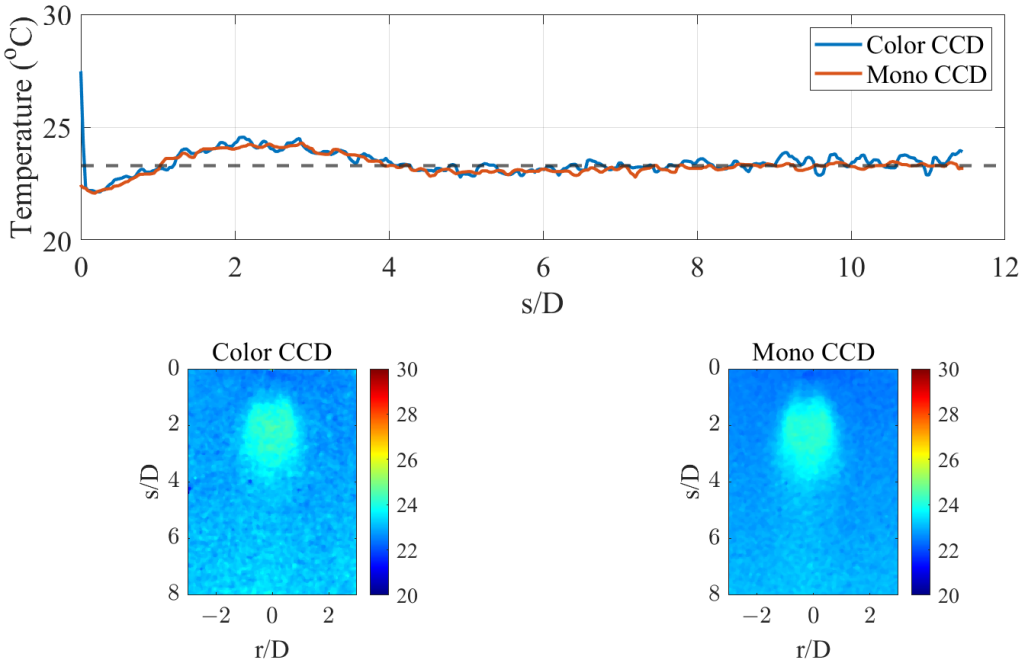

Figure 11. Temperature distribution on the surface and temperature along the centerline at $\alpha = 20°$ and $\Phi = 3.40$.

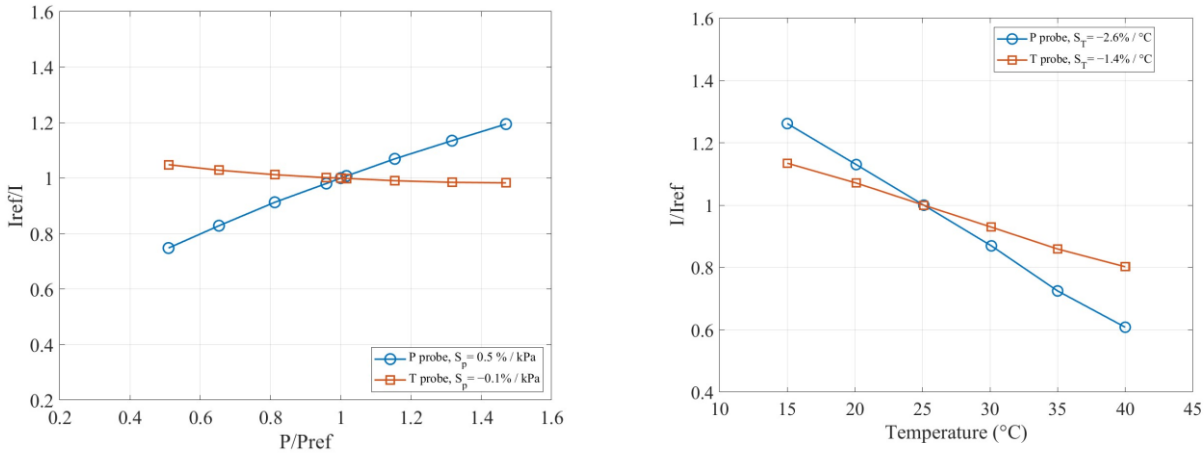

(**a**) (**b**)

Figure 12. Calibration curves of two-color PSP from color CCD camera. (**a**) Pressure calibration and (**b**) temperature calibration.

3.2. Jet Impingement

Pronounced temperature variations are generally present in jet impingement; this complicates the conduct of experiments with traditional PSP with temperature dependency. With the use of a two-color PSP, the error induced by temperature fluctuations can be corrected. The effects of temperature on pressure results are compensated for by using the readings from the temperature probe. Figure 13 illustrates the pressure along the jet centerline, both corrected and uncorrected, at a pressure ratio of 3.40 and an impingement angle of 20° for comparison. In the range of s/D = 0 to 1.5, no apparent differences between corrected and uncorrected pressure readings were discernible. However, the pressure appeared to be higher prior to correction, following the initial pressure wave. This discrepancy was because the temperature began increasing after the first pressure wave, intensifying the temperature effect. Consequently, the intensity of the region diminished, leading to an elevation in pressure. In this context, the pressure appears to have been corrected using the temperature probe data after the pressure waves. Though the correction process introduces some noise, which was originally embedded in the temperature data, the results remain sufficiently clear for analysis.

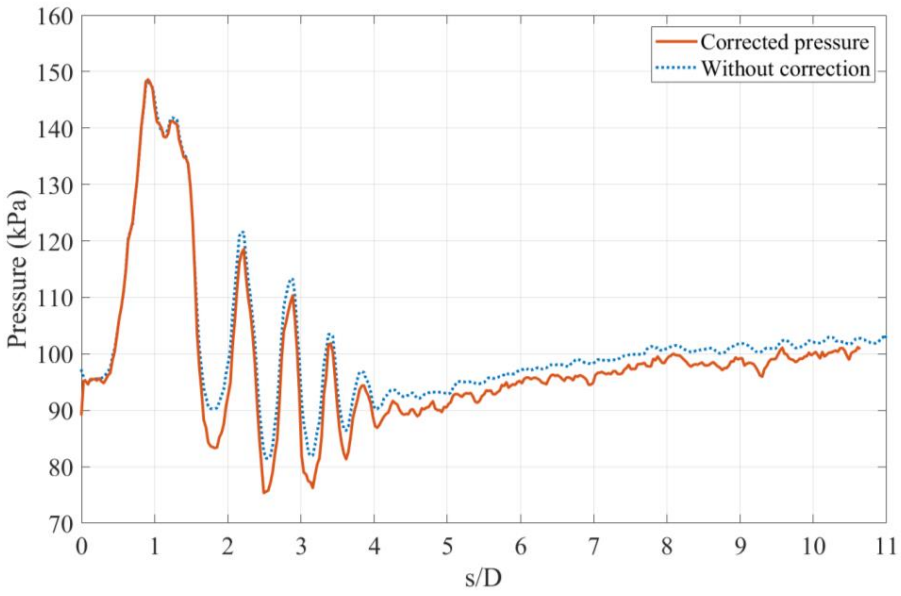

Figure 13. Pressures along the jet centerline corrected and not corrected at $\alpha = 20°$ and $\Phi = 3.40$.

The pressure distribution on the surface at three different pressure ratios (2.38, 3.40, and 4.42) and angles (15°, 20°, and 30°) are depicted in Figures 14–16. These configurations consistently feature an expansion region and a sequence of shock waves. It is noted that the pressure values above 130 kPa are estimated by the extrapolation from the calibration, and the highly extrapolated results might introduce inaccuracy. In Figures 14 and 15, when the pressure ratio is lower, the expansion region encompasses two high-pressure regions. As the angle and pressure ratio increase, these two high-pressure regions move closer to each other. Conversely, at a pressure ratio of 4.42 and an angle of 30°, the expansion region contains only one high-pressure area, indicating that the two high-pressure regions have merged. Simultaneously, the area of the jet extends to both sides, and the maximum pressure increases as the pressure ratio increases. At an angle of 15°, the positions of the maximum pressure are at s/D ratios of 1.86, 1.51, and 1.54 for the three pressure ratios. These results demonstrate that the location of the maximum pressure is independent of the pressure ratio. As the pressure ratio and angle increase, the jet flow shifts closer to the exit of the nozzle. Downstream, the region of the shock waves extends further, and the pressure gradients across the shock waves diminish. The maximum pressure rises with the angle, and the positions of maximum pressure are located in the expansion regions. When the jet operates at the same pressure ratio, the maximum pressure zone shape changes from a fan shape to a round shape as the angle increases. Simultaneously, the shape of the subsequent pressure wave, following the maximum pressure zone, is a crescent shape. This pressure change is also observable in the pressure distribution along the centerline of the jet at different angles, as shown in Figures 17–19. At a pressure ratio of 4.42, the maximum pressures are 136.78, 158.06, and 233.48 kPa at angles of 15°, 20°, and 30°, respectively. Figure 19 reveals that the influence from the flow is focused on the region from the nozzle exit to s/D at 5, leveling off at ambient pressure thereafter.

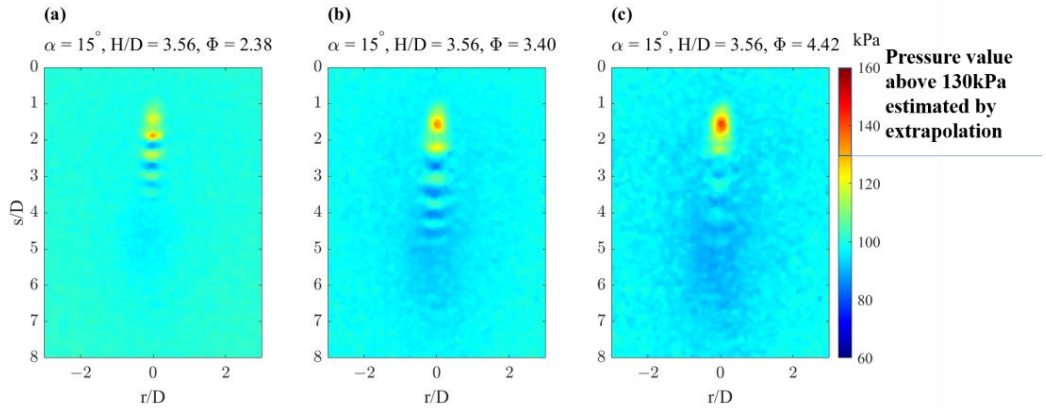

Figure 14. Pressure distribution on the surface at α = 15°.

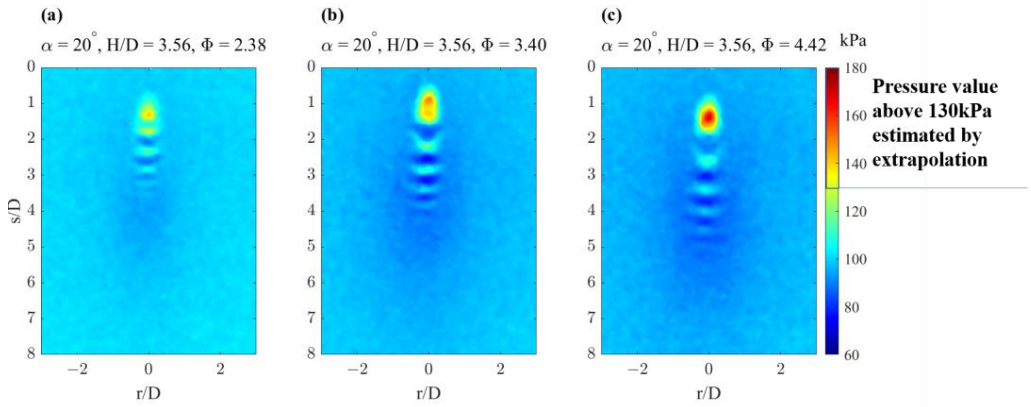

Figure 15. Pressure distribution on the surface at α = 20°.

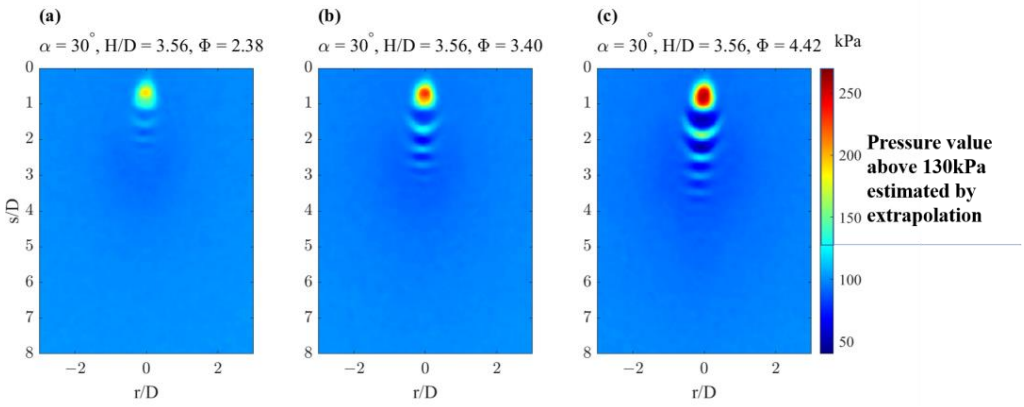

Figure 16. Pressure distribution on the surface at $\alpha = 30°$.

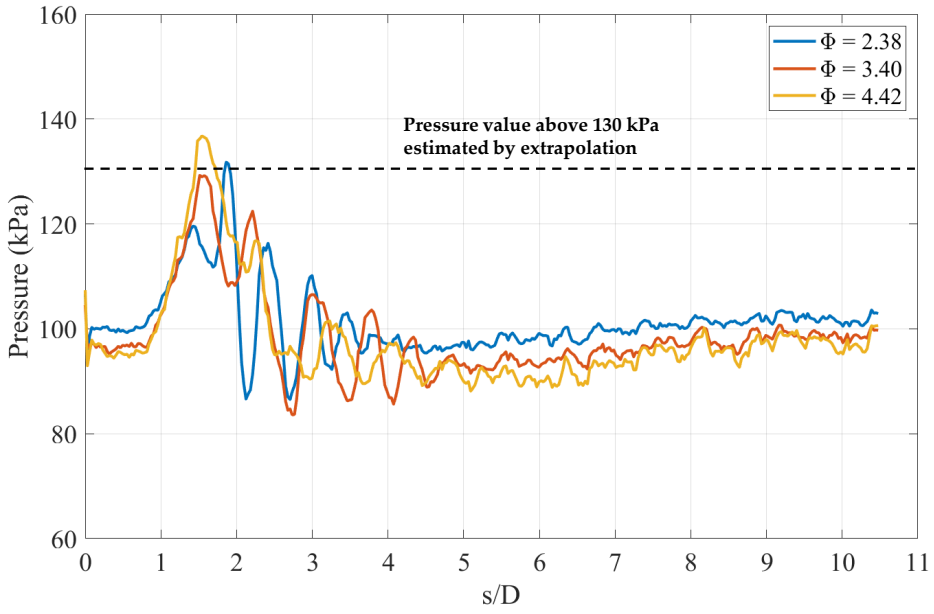

Figure 17. Pressure distribution along the centerline at $\alpha = 15°$.

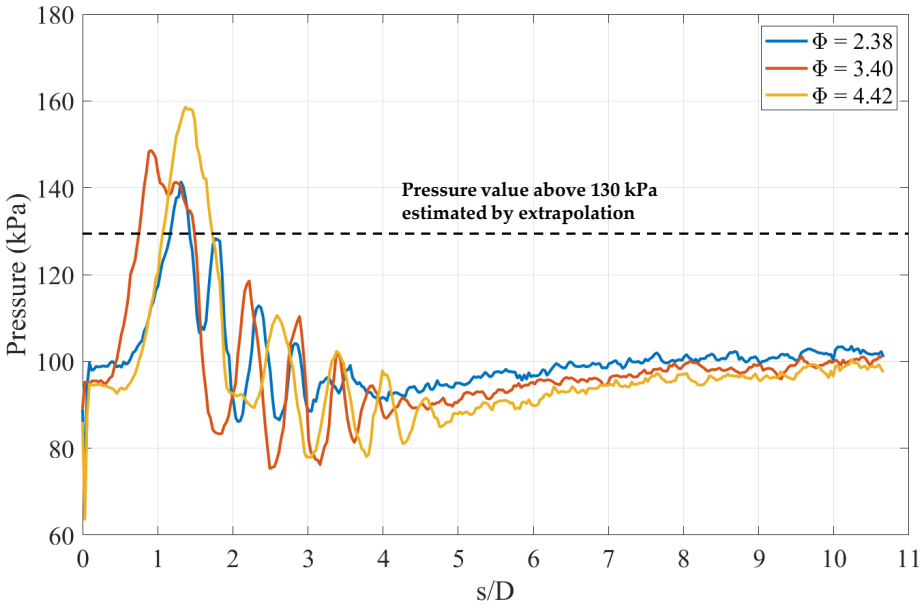

Figure 18. Pressure distribution along the centerline at $\alpha = 20°$.

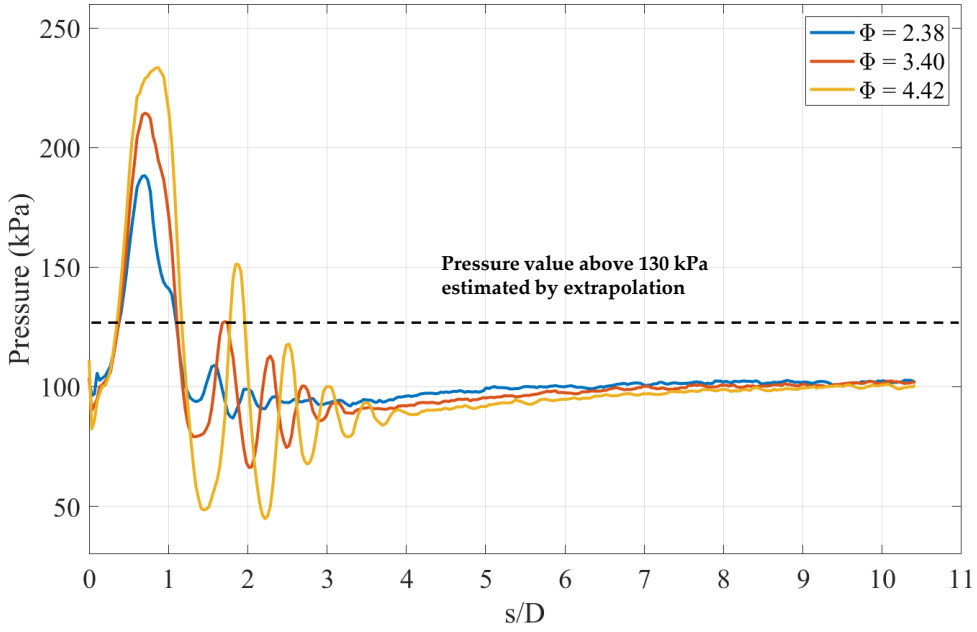

Figure 19. Pressure distribution along the centerline at $\alpha = 30°$.

4. Discussion

The feasibility of the newly developed two-color PSP was demonstrated in this study. The characterization of the luminophores for the development of a two-color PSP led to the selection of PtTFPP and NBD-ZY37 as the pressure and temperature probes, respectively. These probes were chosen due to their stable photodegradation rate, ensuring the maintenance of paint sensitivity without bleaching. Additionally, they exhibit high-pressure sensitivity in the pressure probe and high-temperature sensitivity without pressure dependency in the temperature probe. The temperature dependency of the pressure probe can be adjusted by mixing different binders. However, the two-color PSP remains sensitive to the concentration ratio of the mixing binders, which introduces complexity in balancing the temperature sensitivities in both probes. Thus, a single binder, RTV118, was used in the study. The impingement jet induces a series of shocks and expansion regions, leading to noticeable temperature differences. The two-color PSP has demonstrated effectiveness in impingement experiments for correcting this strong temperature effect. Comparing the corrected and non-corrected pressure data reveals that the errors from temperature variation have been corrected.

This two-color PSP has a limitation that is related to the quantum efficiency in each channel of the color CCD sensor. Despite this, the effect on the pressure calibration of the temperature probe is nonsignificant. Moreover, in comparison to other two-color PSP methods, the preparation and equipment for this technique are as straightforward as those for traditional PSP. With promising temperature sensitivity, the two-color PSP retains considerable potential for application in surface pressure sensing experiments involving temperature variation.

Author Contributions: Conceptualization, W.-C.C. and C.-Y.H.; methodology, W.-C.C., C.-Y.H., K.-T.T. and H.S.; software, W.-C.C. and C.-Y.H.; validation, W.-C.C. and C.-Y.H.; formal analysis, W.-C.C. and C.-Y.H.; investigation, W.-C.C.; resources, C.-Y.H. and K.-T.T.; data curation, W.-C.C.; writing—original draft preparation, W.-C.C.; writing—review and editing, C.-Y.H., K.-T.T. and H.S.; visualization, W.-C.C.; supervision, C.-Y.H.; project administration, W.-C.C.; funding acquisition, C.-Y.H. and H.S. All authors have read and agreed to the published version of the manuscript.

Funding: This research was funded by the National Science and Technology Council, Taiwan: MOST 108-2221-E-007 -030-MY3.

Data Availability Statement: Not applicable.

Conflicts of Interest: The authors declare no conflict of interest.

References

1. Klein, C.; Engler, E.; Henne, U.; Sachs, W. Application of pressure-sensitive paint for determination of the pressure field and calculation of the forces and moments of models in a wind tunnel. *Exp. Fluids* **2005**, *39*, 475–483. [CrossRef]
2. Huang, C.-Y.; Yeh, C.-Y.; Lin, Y.-F.; Chung, K.-M. Global flow visualization of transonic cavity flow with various yaw angles. *Proc. Inst. Mech. Eng. Part G J. Aerosp. Eng.* **2021**, *235*, 1751–1762. [CrossRef]
3. Huang, C.-Y.; Lin, Y.-F.; Huang, Y.-X.; Chung, K.-M. Pressure-sensitive paint measurements with temperature correction on the wing of AGARD-B under transonic flow conditions. *Meas. Sci. Technol.* **2021**, *32*, 094001. [CrossRef]
4. Moon, K.-J.; Mori, H.; Ambe, Y.; Kawabata, H. Development of dual-layer PSP/TSP system for pressure and temperature measurements in low-speed flow field. In Proceedings of the Fluids Engineering Division Summer Meeting, Hamamatsu, Japan, 24–29 July 2011; Volume 44403, pp. 2767–2772.
5. Moon, K.-J.; Mori, H.; Furukawa, M. Simultaneous measurement method of pressure and temperature using dual-layer PSP/TSP with lifetime-based method. *Meas. Sci. Technol.* **2018**, *29*, 125301. [CrossRef]
6. Di, P.; Yingzheng, L. A grid-pattern PSP/TSP system for simultaneous pressure and temperature measurements. *Sens. Actuators B Chem.* **2016**, *222*, 141–150. [CrossRef]
7. Matsuda, Y.; Kameya, T.; Suzuki, Y.; Yoshida, Y.; Egami, Y.; Yamaguchi, H.; Niimi, T. Fine printing of pressure-and temperature-sensitive paints using commercial inkjet printer. *Sens. Actuators B Chem.* **2017**, *250*, 563–568. [CrossRef]
8. Peng, D.; Jensen, C.D.; Juliano, T.J.; Gregory, J.W.; Crafton, J.; Palluconi, S.; Liu, T. Temperature-Compensated Fast Pressure-Sensitive Paint. *AIAA J.* **2013**, *51*, 2420–2431. [CrossRef]
9. Bitter, M.; Wartzek, F.; Übelacker, S.; Schiffer, H.-P.; Kähler, C. Characterization of a Distorted Transonic Compressor Flow using Dual-Luminophore Pressure-Sensitive Paint. In Proceedings of the 10th Pacific Symposium on Flow Visualization and Image Processing (PSFVIP-10), fedOA (Federico II Open Archive), Naples, Italy, 15–18 June 2015.
10. Sachiko, S.; Takahiro, Y.; Tsuyoshi, H.; Katsuaki, M.; Hirotaka, S.; Satoshi, A.; Hidetoshi, M.; Tsuyoshi, M. Temperature compensation of pressure-sensitive luminescent polymer sensors. *Sens. Actuators B Chem.* **2018**, *255*, 1960–1966. [CrossRef]
11. Iijima, Y.; Sakaue, H. Platinum porphyrin and luminescent polymer for two-color pressure- and temperature-sensing probes. *Sens. Actuators A Phys.* **2012**, *184*, 128–133. [CrossRef]
12. Li, X.; Liu, X.; Liu, Y.; Peng, D. Experimental study of near-wall underexpanded jet impingement on a flat plate using temperature-insensitive semi-transparent pressure-sensitive paint. *Exp. Fluids* **2020**, *61*, 232. [CrossRef]
13. Gu, F.; Wei, C.; Liu, Y.; Peng, D.; Liang, L. Temperature sensitivity elimination in sprayable fast-responding pressure-sensitive paint. *Sens. Actuators A Phys.* **2022**, *345*, 113797. [CrossRef]
14. Crafton, J.; Carter, C.; Sullivan, J.; Elliott, G. Pressure measurements on the impingement surface of sonic and sub-sonic jets impinging onto a flat plate at inclined angles. *Exp. Fluids* **2006**, *40*, 697–707. [CrossRef]
15. Chapman, C.; Liu, Y.; Sonek, G.; Tromberg, B. The use of exogenous fluorescent probes for temperature measurements in single living cells. *Photochem. Photobiol.* **1995**, *62*, 416–425. [CrossRef] [PubMed]
16. Fery-Forgues, S.; Fayet, J.-P.; Lopez, A. Drastic changes in the fluorescence properties of NBD probes with the polarity of the medium: Involvement of a TICT state? *J. Photochem. Photobiol. A Chem.* **1993**, *70*, 229–243. [CrossRef]
17. Liu, T.; Sullivan, J.P.; Asai, K.; Klein, C.; Egami, Y. *Pressure and Temperature Sensitive Paints*; Springer: Berlin/Heidelberg, Germany, 2005.